Identification of Tuberculosis based on GCS Method in Image Segmentation

R.Nina Shiny
M.Tech IT
PSN College of Engineering and Technology
selvapoorani@yahoo.co.in

B.Vasantha Chandra
AP / IT
PSN College of Engineering and Technology
vasantha_chandra@yahoo.com

S.Athinarayanan
AP / IT
PSN College of Engineering and Technology

Abstract— Tuberculosis (TB) is the second leading cause of death from an infectious disease worldwide, after HIV. TB is an infectious disease caused by the bacillus Mycobacterium tuberculosis, which typically affects the lungs. Several antibiotics exist for treating TB. While mortality rates are high when left untreated, treatment with antibiotics greatly improves the chances of survival. When left undiagnosed and thus untreated, mortality rates of patients with tuberculosis are high and diagnosing tuberculosis still remains a challenge. An automated approach for detecting tuberculosis in conventional posteroanterior chest radiographs is proposed. First it extracts the lung region using a graph cut segmentation (GCS)method. For this lung region, a set of texture and shape features are computed, which enable the X-rays to be classified as normal or abnormal using a binary classifier. The proposed computer-aided diagnostic system for TB screening, which is ready for field deployment, achieves a performance that approaches the performance of human experts.

***Key Words*— Cross-layer strategies, Markov Decision Process, Reinforcement learning.**

INTRODUCTION

1.1 INTRODUCTON

Tuberculosis is a major health threat in many regions of the world. Opportunistic infections in immunocompromised HIV/AIDS patients and multi-drug-resistant bacterial strains have exacerbated the problem, while diagnosing tuberculosis still remains a challenge. TB is an infectious disease caused by the bacillus Mycobacterium tuberculosis, which typically affects the lungs. It spreads through the air when people with active TB cough, sneeze, or otherwise expel infectious bacteria. Several antibiotics exist for treating TB. While mortality rates are high when left untreated, treatment with antibiotics greatly improves the chances of survival. In clinical trials, cure rates over 90% have been documented. Unfortunately, diagnosing TB is still a major challenge. The definitive test for TB is the identification of Mycobacterium tuberculosis in a clinical sputum or pus sample, which is the current gold standard. However, it may take several months to identify this slow-growing organism in the laboratory. Another technique is sputum smear microscopy, in which bacteria in sputum samples are observed under a microscope. In addition, several skin tests based on immune response are available for determining whether an individual has contracted TB. However, skin tests are not always reliable. The latest development for detection are molecular diagnostic tests that are fast and accurate, and that are highly sensitive and specific.

An automated approach for detecting TB manifestations in chest X-rays (CXRs), based on our earlier work in lung segmentation and lung disease classification is proposed. An automated approach to X-ray reading allows mass screening of large populations that could not be managed manually. A posteroanterior radiograph (X-ray) of a patient's chest is amandatory part of every evaluation for TB. The chest radiograph includes all thoracic anatomy and provides a high yield, given the low cost and single source. Therefore, a reliable screening system for TB detection using radiographs would be a critical step towards more powerful TB diagnostics. It is therefore important to detect patients with TB infections, not only to cure the TB infection itself but also to avoid drug incompatibilities. Medical personnel with little radiology background need to be able to operate the screening system. The target platform for our automated system are portable X-ray scanners, which allow screening of large parts of the population in rural areas. At-risk individuals identified by our system are then referred to a major hospital for treatment.

1.2 FUNDAMENTALS OF MEDICAL IMAGE PROCESSING

Image processing is any form of signal processing for which the input is an image, such as a photograph or video frame; the output of image processing may be either an image or a set of characteristics or parameters related to the image. Most image-processing techniques involve treating the image as a two-dimensional signal and applying standard signal-processing techniques to it.

Medical imaging is the technique, process and art of creating visual representations of the interior of a body for clinical analysis and medical intervention. Medical imaging seeks to reveal internal structures hidden by the skin and bones, as well as to diagnose and treat disease. Medical imaging also establishes a database of normal anatomy and physiology to make it possible to identify abnormalities. Although imaging of removed organs and tissues can be performed for medical reasons, such procedures are usually considered part of pathology instead of medical imaging.

As a discipline and in its widest sense, it is part of biological imaging and incorporates radiology which uses the imaging technologies of X-ray radiography, magnetic resonance imaging, medical ultrasonography or ultrasound, endoscopy, elastography, tactile imaging, thermography, medical photography and nuclear medicine functional imaging techniques as positron emission tomography.

Measurement and recording techniques which are not primarily designed to produce images, such as electroencephalography (EEG), magnetoencephalography

(MEG), electrocardiography (EKG), and others represent other technologies which produce data susceptible to representation as a parameter graph *vs.* time or maps which contain information about the measurement locations.

Medical imaging is often perceived to designate the set of techniques that noninvasively produce images of the internal aspect of the body. In this restricted sense, medical imaging can be seen as the solution of mathematical inverse problems. This means that cause (the properties of living tissue) is inferred from effect (the observed signal). In the case of medical ultrasonography, the probe consists of ultrasonic pressure waves and echoes that go inside the tissue to show the internal structure. In the case of projectional radiography, the probe uses X-ray radiation, which is absorbed at different rates by different tissue types such as bone, muscle and fat.

1.3 IMAGE SEGMENTATION

In computer vision, image segmentation is the process of partitioning a digital image into multiple segments (sets of pixels, also known as superpixels). The goal of segmentation is to simplify and/or change the representation of an image into something that is more meaningful and easier to analyze. Image segmentation is typically used to locate objects and boundaries (lines, curves, etc.) in images. More precisely, image segmentation is the process of assigning a label to every pixel in an image such that pixels with the same label share certain characteristics.

The result of image segmentation is a set of segments that collectively cover the entire image, or a set of contours extracted from the image (see edge detection). Each of the pixels in a region are similar with respect to some characteristic or computed property, such as color, intensity, or texture. Adjacent regions are significantly different with respect to the same characteristic(s). When applied to a stack of images, typical in medical imaging, the resulting contours after image segmentation can be used to create 3D reconstructions with the help of interpolation algorithms like marching cubes.

In general, segmentation in medical images has to cope with poor contrast, acquisition noise due to hardware constraints, and anatomical shape variations. Lung segmentation is no exception in this regard. A lung model that represents the average lung shape of selected training masks is incorporated. Then select these masks according to their shape similarity as follows. Linearly align all training masks to a given input CXR. Then, compute the vertical and horizontal intensity projections of the histogram equalized images. To measure the similarity between projections of the input CXR and the training CXRs, use the Bhattacharyya coefficient. Then use the average mask computed on a subset of the most similar training masks as an approximate lung model for the input CXR.

1.4 METRICS ASSOCIATED WITH SEGMENTATION

Segmentation is treated as the classification problem. The classification success is measured as producer's accuracy or completeness (the number of pixels that are correctly assigned to a certain class divided by the total number of pixels of that class in the input data) and user's accuracy or correctness (the number of pixels correctly assigned to a certain class divided by the total numbers of pixels automatically assigned to that class).

The error matrix consists of a series of rows and columns. The headings of the rows and columns are the classes of interest. The columns contain the ground reference data while the rows contain the classified information. "The intersection of the rows and columns summarize the number of sample units of particular class. Numbers not found within the diagonals are errors. Each error that is made can be referred to as an omission error and a commission error. An omission error is an error where a sample (ie. pixels) should have been included in a certain class, but was included in another. Commission errors are when samples are included in a certain class when they shouldn't be. The overall accuracy is determined by summing all of the numbers within the matrices diagonal (correctly identified samples) and dividing by the sum of all the errors (numbers found outside the diagonal).

Another type of accuracy assessment is through Kappa analysis. This is a discrete multivariate technique that produces a K, which is an estimate of Kappa. This statistic is a measure of how well a classification map and the associated reference data agree with each other. This agreement is based on the major diagonal of the error matrix and a chance agreement. Strong agreement occurs if the K is greater than 0.80. Moderate agreement occurs when K values fall between 0.40 and 0.80 and poor agreement occurs with K values less than 0.40.

1.5 SEGMENTATION USING GRAPH CUT METHOD

Segmentation is an important part of image analysis. It refers to the process of partitioning an image into multiple segments. More precisely, image segmentation is the process of assigning a label to every pixel in an image such that pixels with the same label share certain visual characteristics. The goal of segmentation is to simplify and/or change the representation of an image into something that is more meaningful and easier to analyse. Segmentation can be used for object recognition, occlusion boundary estimation within motion or stereo systems, image compression, image editing, or image database look-up. Segmentation by computing a minimal cut in a graph is a new and quite general approach for segmenting images. This approach guarantees global solutions, which always find best solution, and in addition these solutions are not depending on a good initialization. In our case the segmentation will be based on the image gradient with seeds provided by the user and on the mean intensity of an object.

The paper is organized as follows. The next section gives a survey on lung segmentation. Section 3 highlights the Methodologies. Section 4 highlights the Experimental Evaluation. Finally, Section 5 concludes the paper.

LITERATURE SURVEY

2.1. OVERVIEW

Literature survey is done in order to make a feasible study about the existing problems to formalize the organization's requirements. This process forms the basis of software development and validation by understanding the domain for the software as well as required function behavior and performance.

Sema Candemir, Stefan Jaeger, Kannappan Palaniappan, Sameer Antani, and George Thoma in their work of Graph Cut Based Automatic Lung Boundary Detection in Chest Radiographs presents a graph cut based robust lung segmentation method that detects the lungs with high accuracy. The method consists of two stages: (i) average lung shape model calculation, and (ii) lung boundary detection based on graph cut. Preliminary results on public chest x-rays demonstrate the robustness of the method.

Sema Candemir, Kannappan Palaniappan, and Yusuf Sinan Akgul in their work of "Multi-class regularization parameter learning for graph cut image segmentation," claim that l can be learned by local features which hold the regional characteristics of the image. And hence proposed a l estimation system which is modeled as a multi-class classification scheme. Then demonstrated the performance of the approach within graph cut segmentation framework via qualitative results on chest x-rays. Experimental results indicate that predicted parameters produce better segmentation results.

S. Jaeger, A. Karargyris, S. Antani, and G. Thoma, "Detecting tuberculosis in radiographs using combined lung masks," in their work presents an automated approach for detecting TB on conventional posteroanterior chest radiographs. The idea is to provide developing countries, which have limited access to radiological services and radiological expertise, with an inexpensive detection system that allows screening of large parts of the population in rural areas. And it present results produced by our TB screening system. It combines a lung shape model, a segmentation mask, and a simple intensity model to achieve a better segmentation mask for the lung. With the improved masks, we achieve an area under the ROC curve of more than 83%, measured on data compiled within a tuberculosis control program.

T. Xu, I. Cheng, andM.Mandal, "Automated cavity detection of infectious pulmonary tuberculosis in chest radiographs," have validated our technique on 50 chest radiographs (2048 × 2048 resolution, pixel size 0.25 mm, Delft Imaging Systems, The Netherlands) containing in total 50 cavities. These cavities have been manually outlined by three human experts, one chest radiologist and two readers certified to read chest radiographs according to a tuberculosis scoring system. The automatic border segmentations are compared with manual segmentations provided by the readers using Jaccard overlapping measure. The agreement between the automatically determined outlines is comparable to the inter-observer agreement.

M. Freedman, S. Lo, J. Seibel, and C. Bromley, "Lung nodules: Improved detection with software that suppresses the rib and clavicle on chest radiographs," demonstrated possible superiority in the performance of a radiologist who is tasked with detecting actionable nodules and aided by the bone suppression and soft-tissue visualization algorithm of a new software program that produces a modified image by suppressing the ribs and clavicles, filtering noise, and equalizing the contrast in the area of the lungs.

Y. Boykov, O. Veksler, and R. Zabih, "Fast approximate energy minimization via graph cuts," addressed the problem of minimizing a large class of energy functions that occur in early vision. The major restriction is that the energy function's smoothness term must only involve pairs of pixels. And proposed two algorithms that use graph cuts to compute a local minimum even when very large moves are allowed. The first move considered is an α, β swap: for a pair of labels α, β this move exchanges the labels between an arbitrary set of pixels labeled α and another arbitrary set labeled β. Our first algorithm generates a labeling such that there is no swap move that decreases the energy. The second move considered is an -expansion: for a label α , this move assigns an arbitrary set of pixels the label α. Our second algorithm, which requires the smoothness term to be a metric, generates a labeling such that there is no expansion move that decreases the energy. Moreover, this solution is within a known factor of the global minimum. It experimentally demonstrated the effectiveness of our approach on image restoration, stereo and motion.

K. Palaniappan, F. Bunyak, P. Kumar, I. Ersoy, S. Jaeger, K. Ganguli, A. Haridas, J. Fraser, R. Rao, and G. Seetharaman, "Efficient feature extraction and likelihood fusion for vehicle tracking in low frame rate airborne video," developed an interactive low frame rate tracking system based on a derived rich set of features for vehicle detection using appearance modeling combined with saliency estimation and motion prediction. Instead of applying subspace methods to very high-dimensional feature vectors, we tested the performance of feature fusion to locate the target of interest within the prediction window. Preliminary results show that fusing the feature likelihood maps improves detection but fusing feature maps combined with saliency information actually degrades performance.

N. Dalal and B. Triggs, "Histograms of oriented gradients for human detection", show experimentally that grids of Histograms of Oriented Gradient (HOG) descriptors significantly outperform existing feature sets for human detection. And the study influence of each stage of the computation on performance, concluding that fine-scale gradients, fine orientation binning, relatively coarse spatial binning, and high-quality local contrast normalization in overlapping descriptor blocks are all important for good results. The new approach gives near-

perfect separation on the original MIT pedestrian database, so it introduced a more challenging dataset containing over 1800 annotated human images with a large range of pose variations and backgrounds.

METHODOLOGIES

3.1.SYSTEM OVERVIEW

3.1.1 Existing System

The advent of digital chest radiography and the possibility of digital image processing has given new impetus to computeraided screening and diagnosis. Still, despite its omnipresence in medical practice, the standard CXR is a very complex imaging tool. In the last 10 years, several ground-breaking papers have been published on computer-aided diagnosis (CAD) in CXRs. However, there is no doubt that more research is needed to meet the practical performance requirements for deployable diagnostic systems. In a recent survey, states that 45 years after the initial work on computer-aided diagnosis in chest radiology, there are still no systems that can accurately read chest radiographs. Automated nodule detection is becoming one of the more mature applications of decision support/automation for CXR and CT. Several studies have been published evaluating the capability of commercially available CAD systems to detect lung nodules. The result is that CAD systems can successfully assist radiologists in diagnosing lung cancer. However, nodules represent only one of many manifestations of TB in radiographs. In recent years, due to the complexity of developing fullfledged CAD systems for X-ray analysis, research has concentrated on developing solutions for specific subproblems. The segmentation of the lung field is a typical task that any CAD system needs to support for a proper evaluation of CXRs. Other segmentations that may be helpful include the segmentation of the ribs, heart, and clavicles. Lung segmentation methods including active shapes, rule-based methods, pixel classification, and various combinations thereof exist.

3.1.2 Proposed System

Tuberculosis (TB) is the second leading cause of death from an infectious disease worldwide, after HIV. TB is an infectious disease caused by the bacillus Mycobacterium tuberculosis, which typically affects the lungs. Several antibiotics exist for treating TB. While mortality rates are high when left untreated, treatment with antibiotics greatly improves the chances of survival. When left undiagnosed and thus untreated, mortality rates of patients with tuberculosis are high and diagnosing tuberculosis still remains a challenge. An automated approach for detecting tuberculosis in conventional posteroanterior chest radiographs is proposed. First it extracts the lung region using a graph cut segmentation method. For this lung region, a set of texture and shape features are computed, which enable the X-rays to be classified as normal or abnormal using a binary classifier. The proposed computer-aided diagnostic system for TB screening, which is ready for field deployment, achieves a performance that approaches the performance of human experts.

3.1.3 Graph Cut Based Lung Segmentation

The proposed work implements methods for lung segmentation, feature computation, and classification. First, our system segments the lung of the input CXR using a graph cut optimization method in combination with a lung model. For the segmented lung field, our system then computes a set of features as input to a pre-trained binary classifier. Finally, using decision rules and thresholds, the classifier outputs its confidence in classifying the input CXR as a TB positive case.

The proposed work of lung segmentation is modeled as an optimization problem that takes properties of lung boundaries, regions, and shapes into account. In general, segmentation in medical images has to cope with poor contrast, acquisition noise due to hardware constraints, and anatomical shape variations. Lung segmentation is no exception in this regard. It also incorporates a lung model that represents the average lung shape of selected training masks. Then it selects these masks according to their shape similarity as follows. First linearly aligns all training masks to a given input CXR. Then, it computes the vertical and horizontal intensity projections of the histogram equalized images. To measure the similarity between projections of the input CXR and the training CXRs, we use the Bhattacharyya coefficient. Then it used the average mask computed on a subset of the most similar training masks as an approximate lung model for the input CXR. In particular, we use a subset containing the five most similar training masks to compute the lung model. This empirical number produced the best results in our experiments. Increasing the subset size to more than five masks will decrease the lung model accuracy because the shapes of the additional masks will typically differ from the shape of the input X-ray.

In a second step, it has been employed a graph cut approach and model the lung boundary detection with an objective function. To formulate the objective function, it is defined three requirements a lung region has to satisfy: 1) the lung region should be consistent with typical CXR intensities expected in a lung region, 2) neighboring pixels should have consistent labels, and 3) the lung region needs to be similar to the lung model that has been computed.

According to our method, the optimal configuration of f is given by the minimization of the following objective function:

$$E(f) = E_d(f) + E_s(f) + E_m(f)$$

where Ed , Es , Em represent the region, boundary, and lung model properties of the CXR, respectively. Our average lung model is a 2-D array which contains the probabilities of a pixel p being part of the lung field. Using the three energy terms given above, minimize the objective function with a fast implementation of min-cut/max-flow algorithm.

3.1.4 Features

To describe normal and abnormal patterns in the segmented lung field, it has been experimented with two different feature sets.

3.1.4.1 Object Detection Inspired Features

This method used features that have successfully applied to microscopy images of cells for which they are classified the cell cycle phase based on appearance patterns.

The first set is a combination of shape, edge, and texture descriptors. For each descriptor, it computes a histogram that shows the distribution of the different descriptor values across the lung field. Each histogram bin is a feature, and all features of all descriptors put together form a feature vector that is the input to our classifier. Through empirical experiments, it is found that using 32 bins for each histogram gives us good practical results. In particular, it used the following shape and texture descriptors.

- Intensity histograms (IH).
- Gradient magnitude histograms (GM).
- Shape descriptor histograms (SD)
- Curvature descriptor histograms (CD)
- Histogram of oriented gradients (HOG)
- Local binary patterns (LBP)

3.1.4.2 CBIR-Based Image Features

For our second feature set, Set B, we use a group of low-level features motivated by content-based image retrieval (CBIR). This feature collection includes intensity, edge, texture and shape moment features, which are typically used by CBIR systems. The entire feature vector has 594 dimensions, which is more than three times larger than the feature vector of Set A, and which allows us to evaluate the effect of high- dimensional feature spaces on classification accuracy. We extract most of the features, except for Hu moments and shape features, based on the Lucene image retrieval library.

3.1.5 Classification

To detect abnormal CXRs with TB, we use a support vector machine (SVM), which classifies the computed feature vectors into either normal or abnormal. An SVM in its original form is a supervised nonprobabilistic classifier that generates hyperplanes to separate samples from two different classes in a space with possibly infinite dimension. The unique characteristic of an SVM is that it does so by computing the hyperplane with the largest margin; i.e., the hyperplane with the largest distance to the nearest training data point of any class. Ideally, the feature vectors of abnormal CXRs will have a positive distance to the separating hyperplane, and feature vectors of normal CXRs will have a negative distance. The larger the distance the more confident we are in the class label. Therefore it used these distances as confidence values to compute the ROC curves.

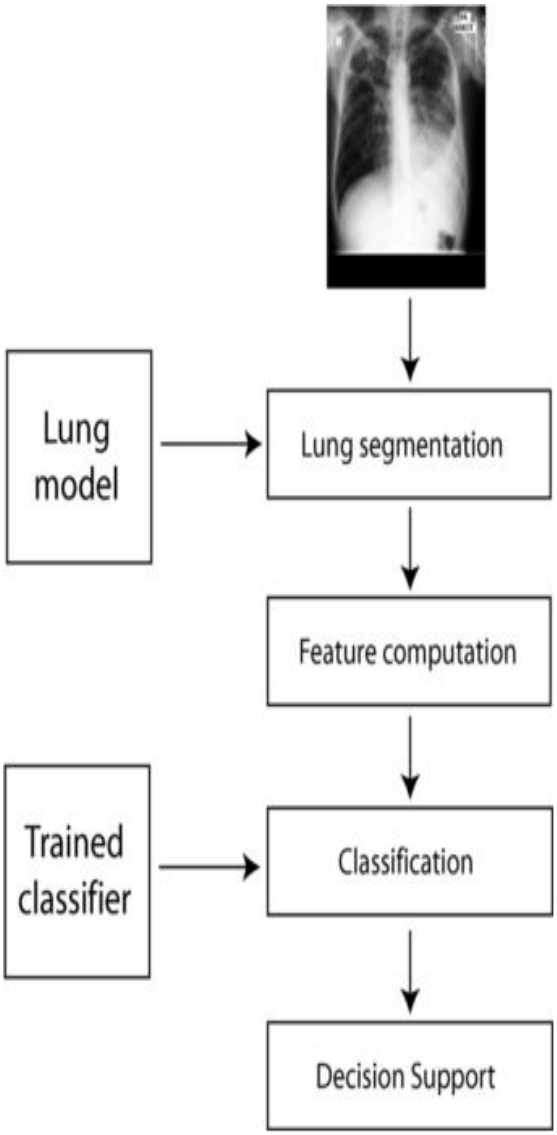

Fig: 3.1 System Architecture

IV. EXPERIMENTAL EVALUATION

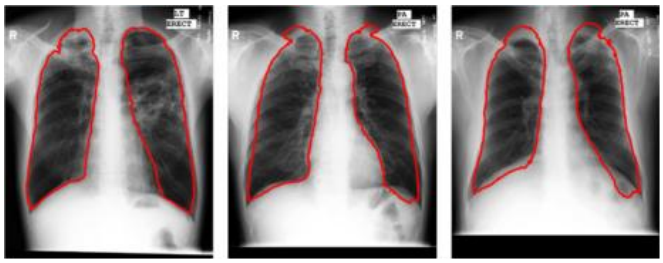

Fig4.3.1 Example lung segmentations for MC CXRs. Note the over-segmentation in the apices. The CXR on the left-hand side has irregular infiltrates in the left lung. The CXR in the middle has small noncalcified nodules in the upper lobes. Grouped noncalcified nodules are visible in the CXR on the right-hand side.

Fig. 4.3.1 shows three examples of our lung segmentation applied to CXRs from the MC dataset. The leftmost CXR has calcifications in the right upper lung and extensive irregular infiltrates in the left lung with a large area of cavitation. The CXR in the middle of Fig. 4.3.1 shows scars in the right upper lung, and the rightmost CXR has scars in the left upper lung and some infiltrates as well. Fig. 4.3.1 also shows the outlines of our segmentation masks for all three lungs. It can be noticed that the segmentation masks capture the general shape of the lungs. Due to the use of a lung model, the infiltrates have not impaired the quality of the segmentations, especially in the leftmost CXR. Again it can be seen a slight leakage of the segmentation in the apical regions for the second and thirdCXR. The lower outlines toward the diaphragm could also be tighter in these images.

As performance measure, the overlap measure Ω is used

$$\Omega = (TP / (TP + FP + FN))$$

where TP is the correctly identified lung area (true positive), FP is the incorrectly identified lung area (false positive), and FN is the missed lung area (false negative). Our segmentation performance is 4.5% lower than the human performance reported for the JSRT set, which is 94.6%.

V. CONCLUSION AND FUTURE WORK

An automated system that screens CXRs for manifestations of TB is developed. When given a CXR as input, our system first segments the lung region using an optimization method based on graph cut. This method combines intensity information with personalized lung atlas models derived from the training set. It computes a set of shape, edge, and texture features as input to a binary classifier, which then classifies the given input image into either normal or abnormal.

To improve the performance further, one approach would be to find optimal weights for the terms in the graph cut energy function. Another possibility would be to use more atlas-based lung models for computing the average lung model. It is surprising that a relatively high performance is achieved when compared to other approaches by using only global features. This may indicate that the combination of local features in the literature is still suboptimal.

REFERENCES

1. S. Candemir, S. Jaeger, K. Palaniappan, S. Antani, and G. Thoma, "Graph-cut based automatic lung boundary detection in chest radiographs," in *Proc. IEEE Healthcare Technol. Conf.: Translat. Eng. Health Med.*, 2012, pp. 31–34.
2. S. Candemir, K. Palaniappan, and Y. Akgul, "Multi-class regularization parameter learning for graph cut image segmentation," in Proc. Int. Symp. Biomed. Imag., 2013, pp. 1473–1476.
3. S. Jaeger, A. Karargyris, S. Antani, and G. Thoma, "Detecting tuberculosis in radiographs using combined lung masks," in Proc. Int. Conf. IEEE Eng. Med. Biol. Soc., 2012, pp. 4978–4981.
4. T. Xu, I. Cheng, andM.Mandal, "Automated cavity detection of infectious pulmonary tuberculosis in chest radiographs," in Proc. Int. IEEE Eng. Med. Biol. Soc., 2011, pp. 5178–5181.
5. M. Freedman, S. Lo, J. Seibel, and C. Bromley, "Lung nodules: Improved detection with software that suppresses the rib and clavicle on chest radiographs," Radiology, vol. 260, no. 1, pp. 265–273, 2011.
6. Y. Boykov, O. Veksler, and R. Zabih, "Fast approximate energy minimization via graph cuts," IEEE Trans. Pattern Anal. Mach. Intell., vol. 23, no. 11, pp. 1222–1239, Nov. 2001.
7. K. Palaniappan, F. Bunyak, P. Kumar, I. Ersoy, S. Jaeger, K. Ganguli, A. Haridas, J. Fraser, R. Rao, and G. Seetharaman, "Efficient feature extraction and likelihood fusion for vehicle tracking in low frame rate airborne video," in Proc. Int. Conf. Inf. Fusion, 2010, pp. 1–8.
8. N. Dalal and B. Triggs, "Histograms of oriented gradients for human detection," in Proc. Int. Conf. Comp. Vis. Patt. Recognit., 2005, vol. 1, pp. 886–893.
9. L. Chen, R. Feris, Y. Zhai, L. Brown, and A. Hampapur, "An integrated system for moving object classification in surveillance videos," in Proc. Int.

Conf. Adv. Video Signal Based Surveill., 2008, pp. 52–59.
10. X.Wang, T. X. Han, and S. Yan, “An HOG-LBP human detector with partial occlusion handling,” in Proc. Int. Conf. Comput. Vis., 2009, pp. 32–39.
11. T. Ojala, M. Pietikäinen, and T. Mäenpää, “Multiresolution gray-scale and rotation invariant texture classification with local binary patterns,” IEEE Trans. Pattern Anal. Mach. Intell., vol. 24, no. 7, pp. 971–987, Jul. 2002.
12. T. Ojala, M. Pietikäinen, and D. Harwood, “A comparative study of texture measures with classification based on feature distributions,” Pattern Recognit., vol. 29, pp. 51–59, 1996.
13. G. Zhao and M. Pietikainen, “Dynamic texture recognition using local binary patterns with an application to facial expressions,” IEEE Trans. Pattern Anal. Mach. Intell., vol. 29, no. 6, pp. 915–928, Jun. 2007.
14. A. Frangi, W. Niessen, K. Vincken, and M. Viergever, “Multiscale vessel enhancement filtering,” in Proc. MICCAI, 1998, pp. 130–137.
15. A. Hoog, H. Meme, H. van Deutekom, A. Mithika, C. Olunga, F. Onyino, and M. Borgdorff, “High sensitivity of chest radiograph reading by clinical officers in a tuberculosis prevalence survey,” Int. J. Tuberculosis Lung Disease, vol. 15, no. 10, pp. 1308–1314, 2011.
16. F. Bunyak, K. Palaniappan,O. Glinskii, V.Glinskii, V. Glinsky, and V. Huxley, “Epifluorescence-based quantitative microvasculature remodeling using geodesic level-sets and shape-based evolution,” in Proc. Int. Conf. IEEE Eng. Med. Biol. Soc., 2008, pp. 3134–3137.
17. M. Simpson, D. You, M. Rahman, D. Demner-Fushman, S. Antani, and G. Thoma, “ITI’s participation in the ImageCLEF 2012 medical retrieval and classification tasks,” in CLEF 2012 Working Notes, 2012.
18. C.-R. Shyu, M. Klaric, G. Scott, A. Barb, C. Davis, and K. Palaniappan, “GeoIRIS: Geospatial information retrieval and indexing system—Content mining, semantics modeling, complex queries,” IEEE Trans. Geosci. Remote Sens., vol. 45, no. 4, pp. 839–852, Apr. 2007.
19. M. Lux and S. Chatzichristofis, “LIRE: Lucene Image Retrieval: An extensible Java CBIR library,” in Proc. ACM Int. Conf. Multimedia, 2008, pp. 1085–1088.
20. M. Lux, “Content-based image retrieval with LIRE,” in Proc. ACM Int. Conf. Multimedia, 2011, pp. 735–738.